International Journal of
Molecular Sciences

MDPI

Article

ZNF750: A Novel Prognostic Biomarker in Metastatic Prostate Cancer

Manuela Montanaro [1,†], Massimiliano Agostini [1,†], Lucia Anemona [1], Elena Bonanno [1], Francesca Servadei [1], Enrico Finazzi Agrò [2], Anastasios D. Asimakopoulos [2], Carlo Ganini [1], Chiara Cipriani [1,3], Marta Signoretti [3], Pierluigi Bove [1,3], Francesco Rugolo [1], Benedetta Imperiali [1], Gerry Melino [1], Alessandro Mauriello [1,*] and Manuel Scimeca [1,4,5,*]

1 Department of Experimental Medicine, Tor Vergata Oncoscience Research (TOR), University of Rome Tor Vergata, 00133 Rome, Italy
2 Department of Surgical Sciences, Division of Urology, University of Rome Tor Vergata, 00133 Rome, Italy
3 San Carlo di Nancy Hospital, 00165 Rome, Italy
4 San Raffaele University, Via di Val Cannuta 247, 00166 Rome, Italy
5 Faculty of Medicine, Saint Camillus International University of Health Sciences, Via di Sant'Alessandro 8, 00131 Rome, Italy
* Correspondence: alessandro.mauriello@uniroma2.it (A.M.); manuel.scimeca@uniroma2.it (M.S.); Tel.: +39-0620903-934 (A.M.)
† These authors contributed equally to this work.

Abstract: Prostate cancer is the most frequently diagnosed cancer and the fifth leading cause of cancer death among men in 2020. The clinical decision making for prostate cancer patients is based on the stratification of the patients according to both clinical and pathological parameters such as Gleason score and prostate-specific antigen levels. However, these tools still do not adequately predict patient outcome. The aim of this study was to investigate whether ZNF750 could have a role in better stratifying patients, identifying those with a higher risk of metastasis and with the poorest prognosis. The data reported here revealed that ZNF750 protein levels are reduced in human prostate cancer samples, and this reduction is even higher in metastatic samples. Interestingly, nuclear positivity is significantly reduced in patients with metastatic prostate cancer, regardless of both Gleason score and grade group. More importantly, the bioinformatics analysis indicates that ZNF750 expression is positively correlated with better prognosis. Overall, our findings suggest that nuclear expression of ZNF750 may be a reliable prognostic biomarker for metastatic prostate cancer, which lays the foundation for the development of new biological therapies.

Keywords: ZNF750; prostate cancer; metastasis; prognostic biomarker

Citation: Montanaro, M.; Agostini, M.; Anemona, L.; Bonanno, E.; Servadei, F.; Finazzi Agrò, E.; Asimakopoulos, A.D.; Ganini, C.; Cipriani, C.; Signoretti, M.; et al. ZNF750: A Novel Prognostic Biomarker in Metastatic Prostate Cancer. *Int. J. Mol. Sci.* **2023**, *24*, 6519. https://doi.org/10.3390/ijms24076519

Academic Editor: Nicola Facchinello

Received: 8 February 2023
Revised: 24 March 2023
Accepted: 25 March 2023
Published: 30 March 2023

1. Introduction

The prostate is the male gland most affected by tumors, and prostate cancer is the most frequently diagnosed cancer and the fifth leading cause of cancer death among men in 2020 [1]. Remarkably, the lack of specific and sensitive markers often leads to overtreatment of prostate cancer which eventually develops into castration-resistant prostate cancer (CRPC). Several mechanisms for the development of CRPC have been proposed, including increased androgen receptor (AR) expression, AR mutation, emergence of AR splice variants, increased intra-tumoral steroid hormone synthesis, and modulation of co-factor activity [2]. At the first histological diagnosis, about 80% of prostate cancers are localized whereas 20% have spread from the primary mass to regional lymph nodes or to distant organs [1]. The presence of metastasis significantly influences the patients' prognosis. In fact, the 5-year survival rate is about 100% for prostate cancer patients with localized mass and only 30% for those with evidence of tumor metastasis. Thus, the prevention of metastatic lesion formation, as well as the identification of new reliable biomarkers of the metastatic

process, are considered a major health challenge. Given this, recent studies have proposed new markers and/or molecular targets for metastatic prostate cancers [3–9]. However, at present, early biomarkers of metastasis are not available for prostate cancer [10].

Zinc finger (ZNF) proteins are one of the most numerous groups of proteins in the whole human genome [11]. The general zinc finger structural organization is preserved by the zinc ion which arranges cysteine and histidine in different combinations [12]. Among the eukaryotic transcriptional factors, the zinc finger domain is one of the most common DNA-binding motifs found [12]. Originally, ZNFs were only identified for their DNA-binding domains; nevertheless, the subsequently discovered multiple and unique ZNF motifs allow ZNF proteins to bind a wide range of target molecules, including RNA, methylated DNA, and lipids [13]. This suggests their potential role in both physiological and pathological processes [12,14].

Among ZNF proteins, the human zinc finger (C2H2-type) protein ZNF750 is a transcription factor composed of an atypical C2H2 zinc finger motif in the amino terminal domain and two highly conserved PLNLS sequences that are involved in DNA binding and protein–protein interactions (Figure 1).

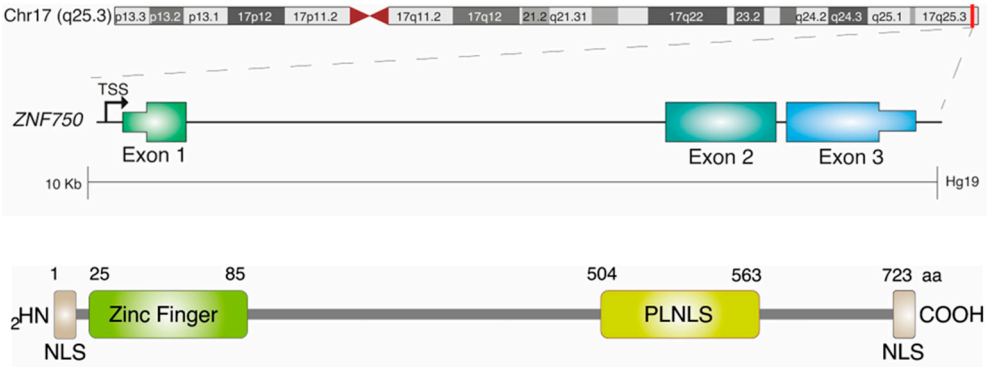

Figure 1. Schematic representation of ZNF750 gene organization and protein structure. ZNF750 gene is located on chromosome 17. The structural organization of ZNF750 consists of an atypical C2H2 zinc finger motif in the amino terminal domain, which is required for the binding of ZNF750 to DNA and regulating gene transcription. In addition, two highly conserved PLNLS sequences that are required for protein–protein interaction are present in the carboxy terminal domain.

ZNF750, by inducing terminal keratinocyte differentiation genes and repressing epidermal progenitor genes, plays a key role in regulating epithelial homeostasis [15,16]. Indeed, mutations within the C2H2 zinc finger motif destroy the ability of ZNF750 to activate differentiation genes, and they have been reported in patients affected by seborrhea-like dermatitis with psoriasiform elements [17]. Moreover, in human squamous cell carcinomas (SCCs) (head and neck, esophagus, cervix, and lung), missense and truncating mutations as well as genomic deletions of the ZNF750 locus have been described [18,19]. In addition, ZNF750 expression is low or undetectable in SCC tissues [20]. Remarkably, these genetic and expression alterations were almost exclusively observed in squamous tumors, highlighting the lineage-specific role of ZNF750 in squamous cancer biology. A low expression level of ZNF750 correlates with a higher incidence of undifferentiated histology and is associated with malignant progression and poor prognosis in SCC patients. We have recently reported that ZNF750 inhibits the migratory and invasive properties of breast cancer cells by recruiting the epigenetic platform KDM1A/HDAC1 to the genetic loci of LAMB3 and CTNNAL1, ultimately repressing their expression [21,22].

Although it has already been recognized that prostate cancer progression is dependent on the ability of p63 to control EMT, a process that occurs in different types of cancer and is regulated by multiple mechanisms (i.e., other members of the p53 family or redox regulators), in the last decade several genomic studies focused on the genomic landscape of primary prostate cancer in order to identify other alterations potentially involved in

tumor progression [23–68]. Large chromosomal rearrangements affecting either the most common tumor suppressor gene, including p53 and PTEN, or oncogene, including c-Myc, have been described [23,51]. In addition, several distinct genomic alterations such as ETV1, ETV4, SPOP, FOXA1, and IDH1 are also present in prostate cancer [52]. More recently, a data-driven deep learning approach found that the genes ADIRF, SLC2A5, C3orf86, and HSPA1B are among the most significant prostate cancer biomarkers [53].

However, at the state of art, only a few biomarkers are used to stratify patients according to the risk of developing metastatic lesions or to predict the most appropriate therapeutic strategy in order to optimize the biological response [54].

Starting from all these considerations, we have hypothesized a possible role for ZNF750 in prostate cancer. Specifically, the aim of this study was to investigate whether ZNF750 could have a role in better stratifying patients, identifying those with a higher risk of metastasis and with the poorest prognosis.

2. Results

2.1. Clinical Features of the Patient Cohort

The mean age of the enrolled patients was 69.8 ± 4.1 for patients with hyperplasia and 72.6 ± 4.8 for patients with acinar prostatic adenocarcinomas. No significant differences were observed.

Metastases were reported in 17 cases (39.5%). In 14 cases, both lymph node and bone metastases were present, while in the remaining 3 cases only bone metastases were observed. As shown in Table 1, metastatic lesions were observed in 5.9% of biopsies classified as grade group 1, 11.8% in grade group 2, 17.6% in grade group 3, and 52.9% and 11.8% in biopsies classified as grade group 4 and 5, respectively.

Table 1. Number of acinar prostatic adenocarcinomas divided at diagnosis by grade group and Gleason score.

Grade Group/Gleason Score	Cases No. (%)	Metastasis No. (%)
1/6 (3 + 3)	4 (9.3%)	1 (5.9%)
2/7 (3 + 4)	13 (30.2%)	2 (11.8%)
3/7 (4 + 3)	7 (16.3%)	3 (17.6%)
4/8 (4 + 4)	17 (39.5%)	9 (52.9%)
5/9 (4 + 5)	2 (4.7%)	2 (11.8%)
Tot.	43 (100%)	17 (100%)

Table 1 also reports the numbers and percentages of metastatic cases according to the Gleason score.

2.2. ZNF750 Expression Is Reduced in Prostate Cancer

The expression of the ZNF750 protein was evaluated by immunohistochemical analysis, and the results are reported in Figure 2 and Table 2.

All patients with benign prostatic hyperplasia (control group) showed marked positivity in all acinar cells. In particular, the intensity of the staining was higher in the nucleus than the cytoplasm. Indeed, ZNF750 positivity was observed in almost all (>80%) nuclei, with a 3+ score, whereas more variability in terms of signal was recorded at the cytoplasmic level, ranging from 40% to 80% of cells, with a 2+/3+ score. Conversely, in prostate acinar carcinomas a significant decrease in ZNF750 positivity in both cytoplasmic and nuclear compartments was observed. Only 6 out of 34 cases showed cytoplasmic positivity (17.6%), whereas 11 samples were completely negative (34.4%) at the nuclear staining. Interestingly, no significant correlation among Gleason score, grade group, and positive or negative ZNF750 cytoplasmic and nuclear expression was noted. However, a positive correlation between the absence of nuclear staining and the presence of metastases was observed ($p = 0.01$). To further confirm the impairment of ZNF750 in prostate cancer, we assessed

the expression of ZNF750 both in a normal prostate epithelial cell line (RWPE1) and in prostate cancer cell lines (PC3 and DU145). As shown in Figure 3A,B, both the mRNA and protein levels of ZNF750 are significantly reduced in prostate cancer cell lines compared to the normal cell line. In addition, as expected, ZNF750 is mainly localized in the nucleus in the normal prostate cell line, in accordance with its function as a transcription factor (Figure 3C).

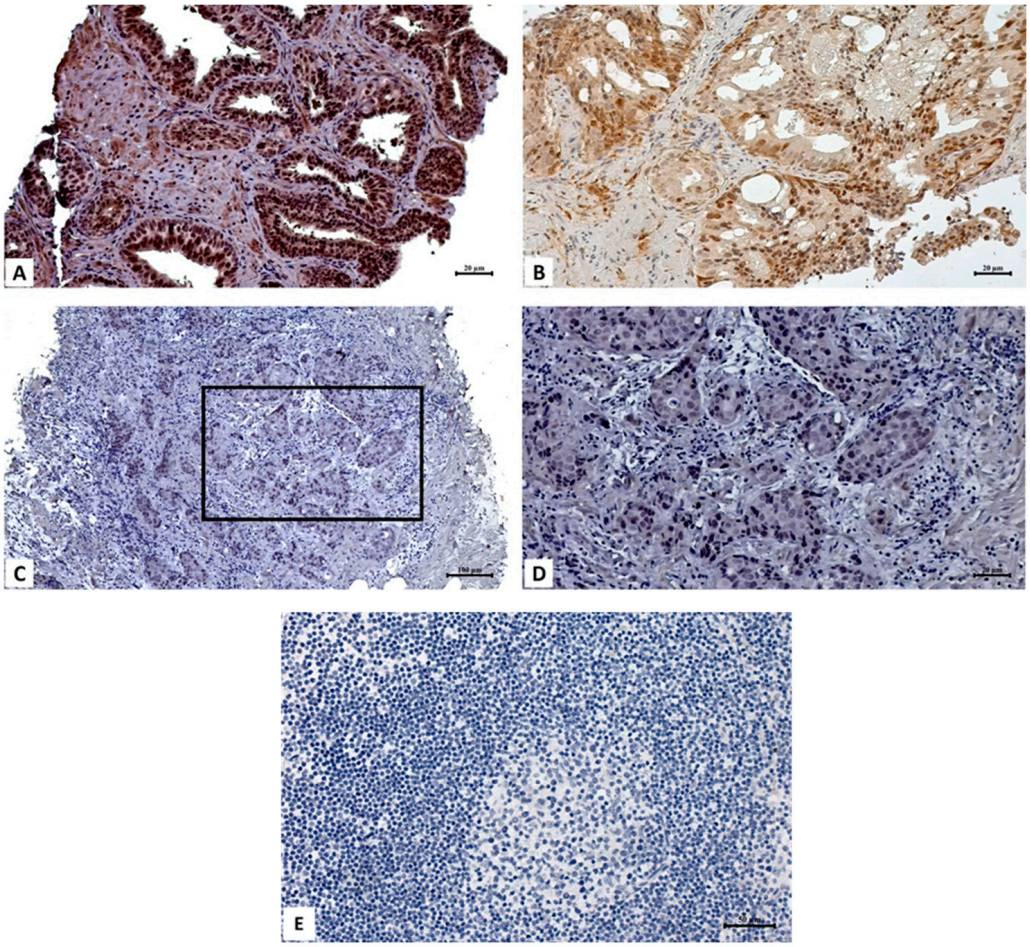

Figure 2. Immunohistochemical analysis. (**A**) Image shows high ZNF750 protein expression in both nucleus and cytoplasm of prostatic hyperplasia cells (scale bar represents 20 μm). (**B**) Non-metastatic prostatic acinar adenocarcinoma, Gleason 8 (4 + 4), characterized by high nuclear and weak cytoplasmic ZNF750 expression (scale bar represents 20 μm). (**C**) No ZNF750 expression in metastatic prostatic acinar adenocarcinoma, Gleason 8 (4 + 4) (scale bar represents 100 μm). Square represents the high magnification in panel (**D**). (**D**) Absence of ZNF750 staining in both nuclear and cytoplasmic compartments (scale bar represents 20 μm). (**E**) ZNF750 staining performed on lymph node tissue as a negative control for ZNF750 immunohistochemical reaction (scale bar represents 50 μm).

Table 2. (A) Evaluation of ZNF750 cytoplasmatic staining in normal prostate and prostatic acinar adenocarcinomas of patients with and without metastasis. (B) Evaluation of ZNF750 nuclear staining in normal prostate and prostatic acinar adenocarcinomas of patients with and without metastasis.

(A)			
	ZNF750 Cytoplasmatic Staining		
	Negative	**Positive**	***p***
Benign Hyperplasia Acinar Carcinoma	0 (0%) 28 (82.4%)	23 (100%) 6 (17.6%)	0.001
Gleason Score			
6	2 (5.8%)	2 (22.2%)	
7	17 (50.0%)	3 (33.3%)	0.33
8	13 (35.4%)	4 (44.5%)	
9	2 (8.8%)	0 (0%)	
Grade Group			
1	2 (5.9%)	2 (22.2%)	
2	12 (35.3%)	1 (11.1%)	0.37
3	5 (14.7%)	2 (22.2%)	
4/5	15 (44.1%)	4 (44.5%)	
Metastasis			
with	17 (100%)	0 (0%)	0.006
w/o	17 (65.4%)	9 (34.6%)	
(B)			
	ZNF750 Nuclear Staining		
	Negative	**Positive**	***p***
Benign Hyperplasia Acinar Carcinoma	0 (0%) 11 (34.4%)	23 (100%) 21 (65.6%)	0.001
Gleason Score			
6	0 (0%)	4 (12.9%)	
7	4 (33.3%)	16 (51.6%)	0.16
8	6 (50.0%)	10 (32.3%)	
9	2 (16.7%)	1 (3.2%)	
Grade Group			
1	0 (0%)	4 (12.9%)	
2	3 (25.0%)	10 (32.3%)	0.09
3	1 (8.3%)	6 (19.3%)	
4/5	8 (66.7%)	11 (35.5%)	
Metastasis			
with	10 (58.8%)	7 (41.2%)	0.01
w/o	2 (7.7%)	24 (92.3%)	

2.3. Loss of ZNF750 Nuclear Expression Predicts Risk of Metastatic Prostate Cancer

Logistic regression analysis was applied to identify the risk of prostate cancer metastasis formation associated with the Gleason score, grade group, and absence of ZNF750 nuclear staining. It should also be highlighted that the absence of ZNF750 expression is a risk factor for metastases, regardless of both Gleason score and grade group. Indeed, as reported in Table 3, the odds ratio for the metastases was about 13-fold compared to both Gleason score and grade group; these risks are significantly higher than the traditional predictive risk factors.

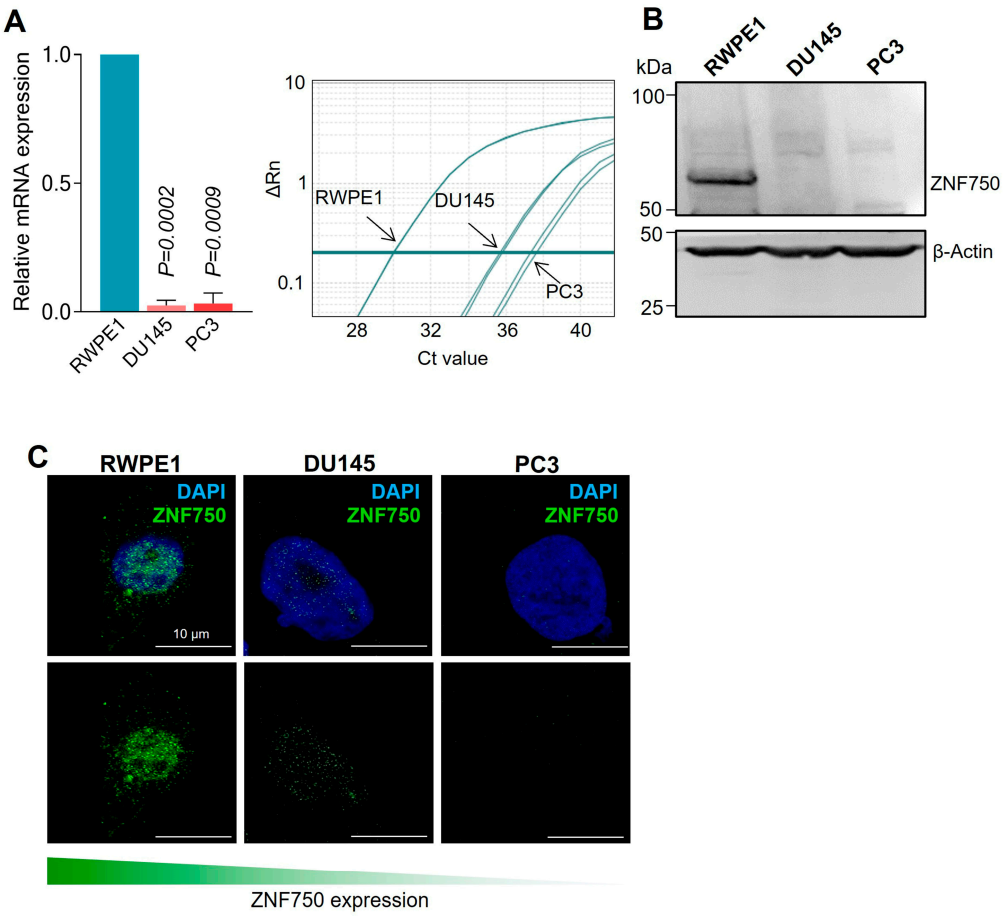

Figure 3. ZNF750 expression is reduced in prostate cancer cell lines. (**A**) ZNF750 mRNA expression in the indicated cell lines assessed by real-time PCR assay. (**B**) ZNF750 protein levels were evaluated by Western blot. A representative image of three independent experiments is shown. (**C**) Confocal microscopy analysis showing that ZNF750 is mainly located in the nucleus of normal prostate epithelial cells. Bars represent means ± SD of three independent experiments.

Table 3. Odds ratio of risk of metastasis in patients with prostatic acinar adenocarcinomas.

	p	Odds Ratio (EXPB)	95% C.I.
Grade Group	0.10	1.89	0.88–4.10
Absence of ZNF750 nuclear positivity	0.005	13.40	2.22–80.81
Gleason Score	0.33	1.70	0.58–4.98
Absence of ZNF750 nuclear positivity	0.004	13.71	2.32–81.02

2.4. Low Levels of ZNF750 Are Associated with a Worse Prognosis

The results obtained from our patient cohort suggest that ZNF750 expression is reduced in patients affected by prostate cancer compared to the control group. To further support these results, a bioinformatics analysis using publicly available datasets of prostate cancer patients was performed. According to our results, the bioinformatics analysis showed that ZNF750 expression is significantly lower ($p = 8.25 \times 10^{-12}$) in both primary and metastatic tumors compared to normal tissues (Figure 4A,B). Interestingly, the bioinformatics analysis indicates that the promoter region of the ZNF750 gene is significantly hypermethylated ($p = 4.58 \times 10^{-9}$) in patients affected by prostate cancer, suggesting that one possible mechanism responsible for the downregulation of ZNF750 in cancer is the methylation of the promoter (Figure 4C). However, the levels of ZNF750 promoter methy-

lation are comparable between the cell lines tested (Figure 4D), suggesting that alternative molecular mechanisms are responsible for the downregulation of ZNF750 expression in prostate cancer cell lines.

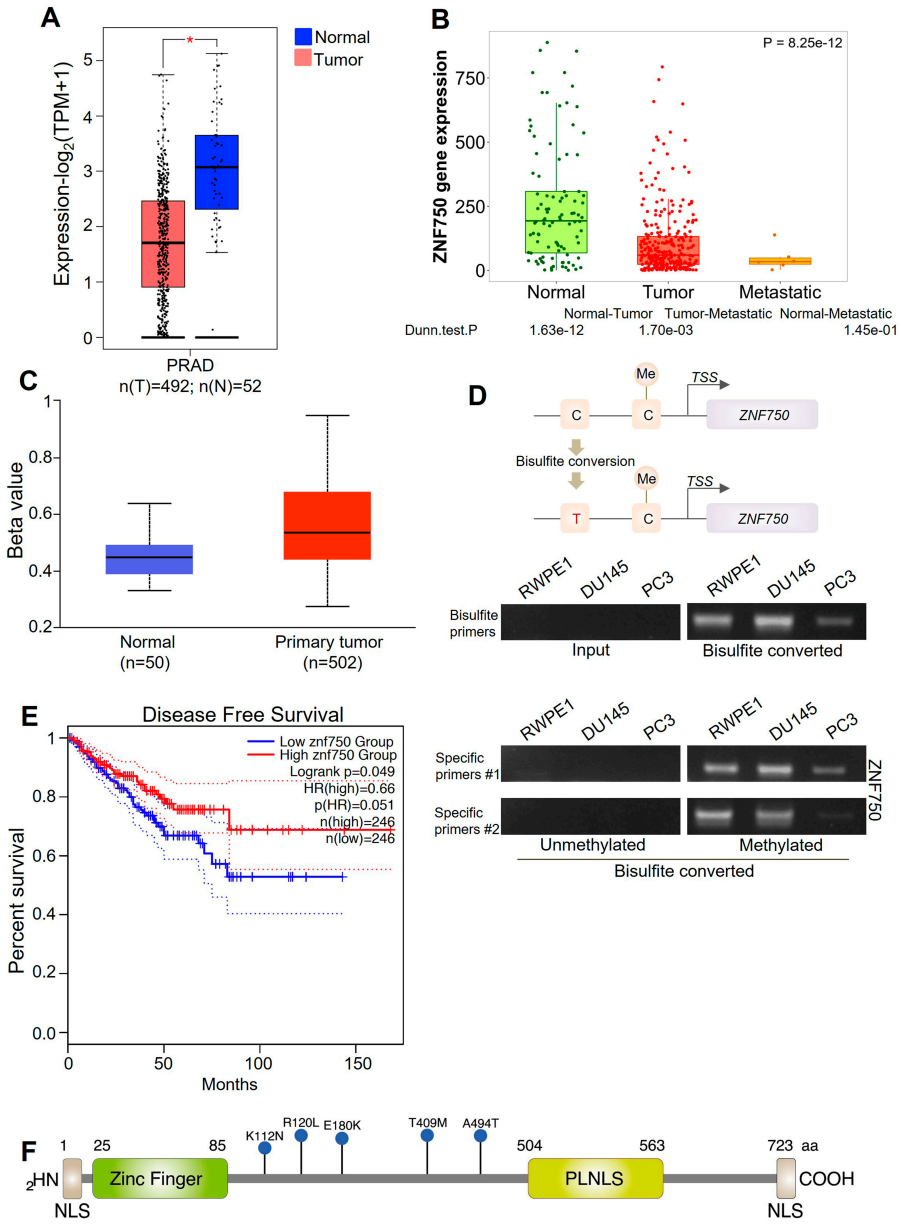

Figure 4. Bioinformatics analysis. (**A**) ZNF750 mRNA expression in tumoral (red, n = 492) and normal (blue, n = 52) tissues, http://gepia.cancer-pku.cn/index.html (accessed on 15 December 2022). * *p*-value < 0.05 (**B**) Differential expression of ZNF750 mRNA in normal (n = 106), tumor (n = 283), and metastatic tissues (n = 6) in prostate cancer, https://tnmplot.com/analysis/ (accessed on 15 December 2022). (**C**) ZNF750 promoter region is methylated in prostatic acinar adenocarcinomas (normal, n = 50 and primary tumor, n = 502). (**D**) ZNF750 promoter methylation status both in normal and cancer cell lines. (**E**) Patients with low expression of ZNF750 mRNA showed a shorter disease-free survival than patients with high expression of ZNF750 (high n = 246 and low n = 246), http://gepia.cancer-pku.cn/index.html (accessed on 15 December 2022). See Section 4 for details of statistical analysis. (**F**) The most common mutations described in human prostate cancer specimen. Blue lollipops indicate the somatic mutations described in human prostate cancer. The analysis was performed using cBioPortal for Cancer Genomics (http://www.cbioportal.org/ (accessed on 15 December 2022)). NLS, nuclear localization.

In human SCCs (head and neck, esophagus, cervix, and lung), missense and truncating mutations as well as genomic deletions of the ZNF750 locus have been described [18,20]. Therefore, we asked whether in prostate cancer ZNF750 results also mutated. To assess the correlation between the expression of ZNF750 and the disease-free survival rate, the GEPIA Dataset was queried. As shown in Figure 4E, low levels of ZNF750 expression are associated with worse disease-free survival. By querying the cBioPortal website, several mutations throughout ZNF750 were identified [55]. All the mutations described are missense mutations (Figure 4F). However, the frequency of mutation is very low (<1%).

3. Discussion

In this study, for the first time, a significant reduction in ZNF750 protein expression in acinar prostate carcinomas, both at the cytoplasmic and nuclear level, has been demonstrated. More interestingly, the absence of ZNF750 nuclear staining may represent an important prognostic factor, since it is associated with a markedly increased risk of metastasis regardless of the traditional prostate cancer prognostic factors, such as the Gleason score and grade group [56,57]. In particular, our data demonstrated that the loss of ZNF750 nuclear positivity indicated a 13-fold increase in the risk of prostate metastasis formation with respect to both the Gleason score and grade group. Overall, the results reported here suggest that ZNF750 expression could potentially be a novel and reliable prognostic biomarker, which could be used to recognize prostate cancer with metastatic capacity. Specifically, ZNF750 expression decreases with the increase in tumor aggressiveness, with a full impairment in metastatic lesions. Moreover, our bioinformatics analysis points out that ZNF750 is also mutated in prostate cancer (Figure 4F). All the mutations described are missense mutations. However, those mutations are present in a region of the protein that does not contain biologically active domains. Therefore, whether those mutations affect protein stability or other aspects of protein function remains to be explored [58–60]. Another question that still needs to be addressed is which molecular mechanism underlies the loss of ZNF750 expression in cancer. Promoter methylation is one of the main epigenetic mechanisms that plays a significant role in gene silencing [61]. Although the bioinformatics analysis indicates a significant increase in ZNF750 promoter methylation, it should be noted that, according to the literature, the promoter region in normal samples is most likely methylated [62,63]. This consideration is in agreement with the methylation levels observed in our normal prostate epithelial cell lines (RWPE1). In conclusion, at this stage it is very difficult to draw clear conclusions regarding the molecular mechanisms involved in the regulation of ZNF750 expression in cancer. On the other hand, we cannot exclude that DNA methylation does not contribute to the regulation of ZNF750 expression. Indeed, there is experimental evidence indicating that the alteration in DNA methylation in some cancers occurs not at the CpG island within the promoter but at CpG island shores (2 kb distant) [64]. Moreover, additional regulatory mechanisms should also be considered, including promoter sequence variants and m6A-mediated repression of ZNF750 expression [65].

The possible role of ZNF750 as a reliable prognostic biomarker for metastatic prostate cancer is also supported by the literature [66,67]. Indeed, ZNF750 is underexpressed in squamous cell carcinoma, and low levels of ZNF750 are associated with poor survival. In addition, Otsuka et al. revealed that ZNF750 predicts the sensitivity and the response to chemoradiotherapy in esophageal and oral squamous cell carcinoma [66]. Breast cancer shares several biological features such as the hormone dependence for tumor growth, and breast cancer subtypes Luminal A and Luminal B are known to have remarkable biological similarities with prostate cancer [68–71]. We have previously shown that low expression of ZNF750 predicts a worse disease-free survival compared to patients with high expression, independently from the breast cancer histotype [21]. However, it is reasonable to think that assessing only the expression of ZNF750 in prostate cancer samples is not sufficient for predicting patient prognosis. Therefore, it is possible to speculate that ZNF750 may

represent a reliable prognostic biomarker in blood, urine, and formalin-fixed paraffin-embedded prostate tissue, as proposed in recent years [72–74].

4. Materials and Methods

4.1. Case Selection

In this study, 57 consecutive patients, 34 with prostatic acinar carcinoma and 23 with benign prostatic hyperplasia, submitted to prostate mapping biopsy at Rome "Tor Vergata" University Polyclinic were enrolled. The prostate mapping biopsy was performed with at least 16 sample areas of both prostatic lobes. Each fragment was formalin-fixed for 24 h and paraffin-embedded [75]. Serial sections were obtained for morphological and immunohistochemical analysis. For each sample, hematoxylin and eosin staining was performed. The Gleason score and the grade group were assessed according to the 2016 WHO [76]. In addition, according to National Comprehensive Cancer Network clinical practice guidelines (NCCN-g), three general risk groups, based on the prostate-specific antigen (PSA), digital rectal examination (DRE), and biopsy, are recognized to better stratify patients as follows: Low risk: tumor is confined to the prostate, and the PSA is <10 and grade group 1 (Gleason 6). Intermediate risk: tumor is confined to the prostate, and the PSA is between 10 and 20, or grade group 2 or 3 (Gleason 7). This category is often divided into a favorable and unfavorable intermediate risk. High risk: tumor extends outside the prostate, with PSA > 20, or grade group 4 or 5 (Gleason 8 to 10). Lastly, very aggressive tumors are defined as very high risk, in which the tumor has extended into the seminal vesicles (T3b) or the rectum or bladder (T4), or there are multiple biopsy samples with high-grade cancer [77]. Moreover, the tumor size and the presence of lymph node and bone metastases were evaluated. The immunohistochemical study was carried out on serial sections obtained from the most representative primary and secondary Gleason score pattern samples. This study was approved by the Institutional Ethical Committee of the "Policlinico Tor Vergata" (reference number #129.18). Experimental procedures were performed in accordance with The Code of Ethics of the World Medical Association (Declaration of Helsinki). Informed consent was obtained from all subjects involved in the study.

4.2. Cell Culture

All cell lines used were obtained from American Type Culture Collection and maintained at 37 °C in 5% CO_2 in culture medium. Cells were grown using the following medium: PC3, F-12K medium supplemented with 10% FCS (Invitrogen, Waltham, MA, USA) and penicillin/streptomycin 1 U/mL (Gibco, Waltham, MA, USA); DU145, EMEM supplemented with 10% FCS (Invitrogen) and penicillin/streptomycin 1 U/mL (Gibco); and RWPE-1, K-SFM supplemented with bovine pituitary extract (BPE), human recombinant epidermal growth factor (EGF), and penicillin/streptomycin 1 U/mL (Gibco).

4.3. Immunohistochemical Analysis

For each case, the expression of anti-ZNF750 was evaluated in both the tumoral primary and secondary Gleason grade area of patients with and without metastasis and in hyperplastic prostatic tissues. Briefly, sections were deparaffinized and, after antigen retrieval (HIER solution at pH 6; 98 °C for 30 min), were incubated with anti-ZNF750 (dilution 1:40, rabbit, polyclonal, Sigma HPA023012) for 1 h at room temperature. The UltraTek HRP Anti-Polyvalent Staining System (Scytek, 205 South 600 West Logan, WV, USA) was used for detection. In all cases, the percentage of positive cells was evaluated. Specifically, cytoplasmatic and/or nuclear positivity was defined by a 0–3+ scoring, according to the following criteria: score 0, none or exceptional positive cells; score 1+, $\leq$10% positive cells; score 2+, 11–50% positive cells; score 3+, >50% positive cells. Histopathologic examination was independently performed by two different pathologists blinded to the clinical data. Interobserver reliability was >98%.

4.4. RNA Isolation and Quantitative Real-Time PCR

Total RNA from cells was isolated using RNeasy minikit (Qiagen, Hilden, Germany) according to the manufacturer's instructions. RNA samples were treated with RNase-free DNase I (Qiagen), and RNA was quantified using a NanoDrop spectrophotometer (Thermo Scientific, Waltham, MA, USA). Total RNA was reverse-transcribed using Superscript III reverse transcriptase and oligo(dT) primer (Invitrogen) [78,79]. qRT-PCR was performed in ABI PRISM 7000 Sequence Detection System (Applied Biosystem, Waltham, MA, USA) with SYBR green ready mix (Applied Biosystem) and specific primers:

ZNF750 for: 5′-AGCTCGCCTGAGTGTGAC-3′;
ZNF750 rev: 5′-TGCAGACTCTGGCCTGTA-3′;
TBP fwd: 5′-TCAAACCCAGAATTGTTCTCCTTAT-3′;
TBP rev: 5′-CCTGAATCCCTTTAGAATAGGGTAG-3′.

Relative mRNA levels were calculated with the $2^{-\Delta\Delta Ct}$ method after normalization to TATA-binding protein (TBP).

4.5. Confocal Microscopy

Cells were seeded into 12-well plates onto glass coverslips. After 24 h, cells were fixed in 4% paraformaldehyde and then permeabilized with 0.1% Triton X-100. For the blocking step, 3% BSA/PBS solution was used for 1 h. Then, cells were incubated with ZNF750 antibody (HPA023012) for 4 h and diluted 1:250 in 3% BSA/PBS solution. The incubation with the secondary antibody Alexa Fluor® 488 (ab150077) was performed for 1 h and diluted 1:500 in 3% BSA/PBS solution. Nuclei were stained with DAPI for 15 min. The coverslips were then mounted with ProLong™ Gold Antifade Mountant (Thermo Fisher) onto glass slides and observed under a confocal microscope (Leica Stellaris, Wetzlar, Germany) using the 63× objective.

4.6. Promoter Methylation

The promoter methylation analysis was performed using Active Motif's Bisulfite Conversion Kit, following the manufacturer's instructions. Briefly, genomic DNA was extracted from cell lines using the Wizard® Genomic DNA Purification Kit and then quantified with NanoDrop™. Samples were then treated with Proteinase K for 30 min at 50 °C. For the conversion reaction, 2 µg of DNA was used. The quality of the converted product was checked using the PCR Primer Mix provided by the kit. PCR was performed using the REDTaq® ReadyMix™ PCR Reaction Mix. Specific primers for methylated and unmethylated DNA are listed below:

ZNF750 Met F1—TTT ATT TTA ATT GCG GAT ATA TCG A;
ZNF750 Met R1—TTA CAC CCA CCG AAC TAC TAC G;
ZNF750 Unmet F1—TTT ATT TTA ATT GTG GAT ATA TTG A;
ZNF750 Unmet R1—TTT ACA CCC ACC AAA CTA CTA CAA A;
ZNF750 Met F2—TTT ATT TTA ATT GCG GAT ATA TCG A;
ZNF750 Met R2—AC ACC CAC CGA ACT ACT ACG A;
ZNF750 Unmet F2—TTT TTA TTT TAA TTG TGG ATA TAT TGA;
ZNF750 Unmet R2—TTT ACA CCC ACC AAA CTA CTA CAA A.

4.7. Bioinformatics Analysis and Mutational Analysis

To investigate the potential prognostic value of ZNF750, a disease-free survival curve and differential gene expression analysis were performed. Specifically, the GEPIA Dataset and TNMplot tool of the Kaplan–Meier Plotter were employed to compare the expression of the gene in normal prostate, prostatic cancer, and metastasis. GEPIA Dataset included 492 tumoral and 52 normal samples from TCGA data, whereas TNMplot graph refers to 106 normal samples, 283 prostatic cancer tissues, and 6 metastases. The bioinformatics analysis was carried out by using the online available tools: GEPIA, cBioPortal, Kaplan–Meier Plotter, and UALCAN [80–87]. Mutational analysis was carried out using the cBioPortal website [55].

4.8. Statistical Analysis

Data were analyzed using SPSS version 16.0 (SPSS Inc., Chicago, IL, USA) software. Continuous variables were expressed as the mean ± SEM. Categorical data were analyzed using the chi-square test or the Fisher exact test.

The odds ratio for metastasis risks was evaluated for grade group, Gleason score, and ZNF750 expression by logistic regression, using the value of EXP (B), where B represents the logistic coefficient. A 2-tailed p value < 0.05 was considered statistically significant.

For bioinformatics analysis, the following tests were used: gene expression: ANOVA test, Kruskal–Wallis test, and Dunn's test; promoter methylation: Welch's t-test; survival analysis: log-rank test.

5. Conclusions

In conclusion, it is emerging that ZNF750 can potentially act as a prognostic biomarker in cancer and most likely be used to predict the formation of metastasis. Risk assessment is of fundamental importance for clinical decision making. Therefore, a better stratification of patients by both prognostic and predictive factors may lead to a higher-quality management of the disease and to the identification of new therapeutic strategies.

Author Contributions: M.M., M.A. and A.M.: conceptualization; M.M., M.S. (Manuel Scimeca), L.A., F.S., E.F.A., A.D.A., M.S. (Marta Signoretti), B.I. and P.B.: methodology; M.A., F.R. and B.I.: software; M.M., M.A., A.M. and G.M.: data curation; M.M., M.A., M.S. (Manuel Scimeca) and A.M.: writing—original draft preparation; L.A., E.B., P.B., F.S., E.F.A., A.D.A., C.G., C.C., M.S. (Marta Signoretti) and F.R.: writing—review and editing, M.A., F.R., C.G., B.I., M.S. (Marta Signoretti) and C.C.: visualization; G.M. and A.M.: supervision; E.B., M.A. and G.M.: funding acquisition. All authors have read and agreed to the published version of the manuscript.

Funding: This research was funded by "Ricerca Ateneo Beyond Borders" (D. R. n. 1347 del 29 May 2019)—Transcription factor ZNF750 in breast and prostate Adenocarcinoma Progression (CUP# E84I20000650005) to E.B.,"Associazione Italiana per la Ricerca contro il Cancro" (AIRC) to G.M. (IG 2022 ID 27366; 2023–2027) and by Ministry Universities and Research PNRR-PE6-M4C2I1.3 PE6, project PE00000019 Heal Italia grant to G.M., M.A. and A.M.

Institutional Review Board Statement: Not applicable.

Informed Consent Statement: Not applicable.

Data Availability Statement: Bioinformatics data can be found at: http://gepia.cancer-pku.cn/index.html; https://www.cbioportal.org; https://kmplot.com/analysis/; accessed on 15 December 2022. Histological, immunohistochemical, and molecular data will be provided on request.

Conflicts of Interest: G.M. and M.A. are members of the Editorial Board of CDDpress/Springer Nature. The authors declare no other conflict of interest.

References

1. Sung, H.; Ferlay, J.; Siegel, R.L.; Laversanne, M.; Soerjomataram, I.; Jemal, A.; Bray, F. Global Cancer Statistics 2020: GLOBOCAN Estimates of Incidence and Mortality Worldwide for 36 Cancers in 185 Countries. *CA Cancer J. Clin.* **2021**, *71*, 209–249. [CrossRef] [PubMed]
2. Vellky, J.E.; Ricke, W.A. Development and prevalence of castration-resistant prostate cancer subtypes. *Neoplasia* **2020**, *22*, 566–575. [CrossRef]
3. Scimeca, M.; Montanaro, M.; Bonfiglio, R.; Anemona, L.; Agrò, E.F.; Asimakopoulos, A.D.; Bei, R.; Manzari, V.; Urbano, N.; Giacobbi, E.; et al. The ETS Homologous Factor (EHF) Represents a Useful Immunohistochemical Marker for Predicting Prostate Cancer Metastasis. *Diagnostics* **2022**, *12*, 800. [CrossRef] [PubMed]
4. Mapelli, S.N.; Albino, D.; Mello-Grand, M.; Shinde, D.; Scimeca, M.; Bonfiglio, R.; Bonanno, E.; Chiorino, G.; Garcia-Escudero, R.; Catapano, C.V.; et al. A Novel Prostate Cell Type-Specific Gene Signature to Interrogate Prostate Tumor Differentiation Status and Monitor Therapeutic Response (Running Title: Phenotypic Classification of Prostate Tumors). *Cancers* **2020**, *12*, 176. [CrossRef]
5. Urbano, N.; Scimeca, M.; Crocco, A.; Mauriello, A.; Bonanno, E.; Schillaci, O. 18F-Choline PET/CT Identifies High-Grade Prostate Cancer Lesions Expressing Bone Biomarkers. *J. Clin. Med.* **2019**, *8*, 1657. [CrossRef]

6. Scimeca, M.; Bonfiglio, R.; Urbano, N.; Cerroni, C.; Anemona, L.; Montanaro, M.; Fazi, S.; Schillaci, O.; Mauriello, A.; Bonanno, E. Programmed death ligand 1 expression in prostate cancer cells is associated with deep changes of the tumor inflammatory infiltrate composition. *Urol. Oncol.* **2019**, *37*, e19–e297. [CrossRef]
7. Scimeca, M.; Urbano, N.; Bonfiglio, R.; Mapelli, S.N.; Catapano, C.V.; Carbone, G.M.; Ciuffa, S.; Tavolozza, M.; Schillaci, O.; Mauriello, A.; et al. Prostate Osteoblast-Like Cells: A Reliable Prognostic Marker of Bone Metastasis in Prostate Cancer Patients. *Contrast Media Mol. Imaging* **2018**, *2018*, 9840962, Erratum in *Contrast Media Mol. Imaging* **2019**, *2019*, 7843735. [CrossRef] [PubMed]
8. Formosa, A.; Lena, A.M.; Markert, E.K.; Cortelli, S.; Miano, R.; Mauriello, A.; Croce, N.; Vandesompele, J.; Mestdagh, P.; Finazzi-Agrò, E.; et al. DNA methylation silences miR-132 in prostate cancer. *Oncogene* **2013**, *32*, 127–134. [CrossRef]
9. Viticchiè, G.; Lena, A.M.; Latina, A.; Formosa, A.; Gregersen, L.H.; Lund, A.H.; Bernardini, S.; Mauriello, A.; Miano, R.; Spagnoli, L.G.; et al. MiR-203 controls proliferation, migration and invasive potential of prostate cancer cell lines. *Cell Cycle* **2011**, *10*, 1121–1131. [CrossRef]
10. Galazi, M.; Rodriguez-Vida, A.; Ng, T.; Mason, M.; Chowdhury, S. Precision medicine for prostate cancer. *Expert Rev. Anticancer Ther.* **2014**, *14*, 1305–1315. [CrossRef]
11. Singh, J.K.; van Attikum, H. DNA double-strand break repair: Putting zinc fingers on the sore spot. *Semin. Cell Dev. Biol.* **2021**, *113*, 65–74. [CrossRef] [PubMed]
12. Cassandri, M.; Smirnov, A.; Novelli, F.; Pitolli, C.; Agostini, M.; Malewicz, M.; Melino, G.; Raschellà, G. Zinc-finger proteins in health and disease. *Cell Death Discov.* **2017**, *3*, 17071. [CrossRef] [PubMed]
13. Laity, J.; Lee, B.; Wright, P. Zinc finger proteins: New insights into structural and functional diversity. *Curr. Opin. Struct. Biol.* **2001**, *11*, 39–46. [CrossRef] [PubMed]
14. Amelio, I.; Bertolo, R.; Bove, P.; Candi, E.; Chiocchi, M.; Cipriani, C.; Di Daniele, N.; Ganini, C.; Juhl, H.; Mauriello, A.; et al. Cancer predictive studies. *Biol. Direct* **2020**, *15*, 18. [CrossRef]
15. Boxer, L.D.; Barajas, B.; Tao, S.; Zhang, J.; Khavari, P.A. ZNF750 interacts with KLF4 and RCOR1, KDM1A, and CTBP1/2 chromatin regulators to repress epidermal progenitor genes and induce differentiation genes. *Genes Dev.* **2014**, *28*, 2013–2026. [CrossRef]
16. Gatti, V.; Fierro, C.; Compagnone, M.; La Banca, V.; Mauriello, A.; Montanaro, M.; Scalera, S.; De Nicola, F.; Candi, E.; Ricci, F.; et al. ΔNp63-Senataxin circuit controls keratinocyte differentiation by promoting the transcriptional termination of epidermal genes. *Proc. Natl. Acad. Sci. USA* **2022**, *119*, e2104718119. [CrossRef] [PubMed]
17. Birnbaum, R.Y.; Zvulunov, A.; Hallel-Halevy, D.; Cagnano, E.; Finer, G.; Ofir, R.; Geiger, D.; Silberstein, E.; Feferman, Y.; Birk, O.S. Seborrhea-like dermatitis with psoriasiform elements caused by a mutation in ZNF750, encoding a putative C2H2 zinc finger protein. *Nat. Genet.* **2006**, *38*, 749–751. [CrossRef]
18. Lin, D.C.; Hao, J.J.; Nagata, Y.; Xu, L.; Shang, L.; Meng, X.; Sato, Y.; Okuno, Y.; Varela, A.M.; Ding, L.W.; et al. Genomic and molecular characterization of esophageal squamous cell carcinoma. *Nat. Genet.* **2014**, *46*, 467–473. [CrossRef]
19. Nambara, S.; Masuda, T.; Tobo, T.; Kidogami, S.; Komatsu, H.; Sugimachi, K.; Saeki, H.; Oki, E.; Maehara, Y.; Mimori, K. Clinical significance of ZNF750 gene expression, a novel tumor suppressor gene, in esophageal squamous cell carcinoma. *Oncol. Lett.* **2017**, *14*, 1795–1801. [CrossRef]
20. Hazawa, M.; Lin, D.C.; Handral, H.; Xu, L.; Chen, Y.; Jiang, Y.Y.; Mayakonda, A.; Ding, L.W.; Meng, X.; Sharma, A.; et al. ZNF750 is a lineage-specific tumour suppressor in squamous cell carcinoma. *Oncogene* **2017**, *36*, 2243–2254. [CrossRef]
21. Cassandri, M.; Butera, A.; Amelio, I.; Lena, A.M.; Montanaro, M.; Mauriello, A.; Anemona, L.; Candi, E.; Knight, R.A.; Agostini, M.; et al. ZNF750 represses breast cancer invasion via epigenetic control of prometastatic genes. *Oncogene* **2020**, *39*, 4331–4343. [CrossRef] [PubMed]
22. Butera, A.; Cassandri, M.; Rugolo, F.; Agostini, M.; Melino, G. The ZNF750-RAC1 axis as potential prognostic factor for breast cancer. *Cell Death Discov.* **2020**, *6*, 135. [CrossRef]
23. Cancer Genome Atlas Research Network. The Molecular Taxonomy of Primary Prostate Cancer. *Cell* **2015**, *163*, 1011–1025. [CrossRef]
24. Li, J.; Xu, C.; Lee, H.J.; Ren, S.; Zi, X.; Zhang, Z.; Wang, H.; Yu, Y.; Yang, C.; Gao, X.; et al. A genomic and epigenomic atlas of prostate cancer in Asian populations. *Nature* **2020**, *580*, 93–99. [CrossRef] [PubMed]
25. De Laurenzi, V.; Melino, G. Evolution of functions within the p53/p63/p73 family. *Ann. N. Y. Acad. Sci.* **2000**, *926*, 90–100. [CrossRef]
26. Tucci, P.; Agostini, M.; Grespi, F.; Markert, E.K.; Terrinoni, A.; Vousden, K.H.; Muller, P.A.; Dötsch, V.; Kehrloesser, S.; Sayan, B.S.; et al. Loss of p63 and its microRNA-205 target results in enhanced cell migration and metastasis in prostate cancer. *Proc. Natl. Acad. Sci. USA* **2012**, *109*, 15312–15317, Erratum in *Proc. Natl. Acad. Sci. USA* **2014**, *111*, 2855. [CrossRef]
27. Shalom-Feuerstein, R.; Lena, A.M.; Zhou, H.; De La Forest Divonne, S.; Van Bokhoven, H.; Candi, E.; Melino, G.; Aberdam, D. ΔNp63 is an ectodermal gatekeeper of epidermal morphogenesis. *Cell Death Differ.* **2011**, *18*, 887–896. [CrossRef]
28. Deng, G.; Wang, R.; Sun, Y.; Huang, C.P.; Yeh, S.; You, B.; Feng, C.; Li, G.; Ma, S.; Chang, C. Targeting androgen receptor (AR) with antiandrogen Enzalutamide increases prostate cancer cell invasion yet decreases bladder cancer cell invasion via differentially altering the AR/circRNA-ARC1/miR-125b-2-3p or miR-4736/PPARγ/MMP-9 signals. *Cell Death Differ.* **2021**, *28*, 2145–2159. [CrossRef] [PubMed]

29. Velletri, T.; Huang, Y.; Wang, Y.; Li, Q.; Hu, M.; Xie, N.; Yang, Q.; Chen, X.; Chen, Q.; Shou, P.; et al. Loss of p53 in mesenchymal stem cells promotes alteration of bone remodeling through negative regulation of osteoprotegerin. *Cell Death Differ.* **2021**, *28*, 156–169. [CrossRef] [PubMed]
30. Jang, H.R.; Shin, S.B.; Kim, C.H.; Won, J.Y.; Xu, R.; Kim, D.E.; Yim, H. PLK1/vimentin signaling facilitates immune escape by recruiting Smad2/3 to PD-L1 promoter in metastatic lung adenocarcinoma. *Cell Death Differ.* **2021**, *28*, 2745–2764, Erratum in *Cell Death Differ.* **2021**, *29*, 2106. [CrossRef]
31. Gao, J.; Liu, R.; Feng, D.; Huang, W.; Huo, M.; Zhang, J.; Leng, S.; Yang, Y.; Yang, T.; Yin, X.; et al. Snail/PRMT5/NuRD complex contributes to DNA hypermethylation in cervical cancer by TET1 inhibition. *Cell Death Differ.* **2021**, *28*, 2818–2836. [CrossRef]
32. Yang, S.; Li, H.; Yao, H.; Zhang, Y.; Bao, H.; Wu, L.; Zhang, C.; Li, M.; Feng, L.; Zhang, J.; et al. Long noncoding RNA ERLR mediates epithelial-mesenchymal transition of retinal pigment epithelial cells and promotes experimental proliferative vitreoretinopathy. *Cell Death Differ.* **2021**, *28*, 2351–2366. [CrossRef]
33. Li, X.; Yuan, J.; Song, C.; Lei, Y.; Xu, J.; Zhang, G.; Wang, W.; Song, G. Deubiquitinase USP39 and E3 ligase TRIM26 balance the level of ZEB1 ubiquitination and thereby determine the progression of hepatocellular carcinoma. *Cell Death Differ.* **2021**, *28*, 2315–2332. [CrossRef]
34. Ciocci, M.; Mochi, F.; Carotenuto, F.; Di Giovanni, E.; Prosposito, P.; Francini, R.; De Matteis, F.; Reshetov, I.; Casalboni, M.; Melino, S.; et al. Scaffold-in-Scaffold Potential to Induce Growth and Differentiation of Cardiac Progenitor Cells. *Stem Cells Dev.* **2017**, *26*, 1438–1447. [CrossRef] [PubMed]
35. Ganini, C.; Amelio, I.; Bertolo, R.; Bove, P.; Buonomo, O.C.; Candi, E.; Cipriani, C.; Di Daniele, N.; Juhl, H.; Mauriello, A.; et al. Global mapping of cancers: The Cancer Genome Atlas and beyond. *Mol. Oncol.* **2021**, *15*, 2823–2840. [CrossRef]
36. Cabras, T.; Patamia, M.; Melino, S.; Inzitari, R.; Messana, I.; Castagnola, M.; Petruzzelli, R. Pro-oxidant activity of histatin 5 related Cu(II)-model peptide probed by mass spectrometry. *Biochem. Biophys. Res. Commun.* **2007**, *358*, 277–284. [CrossRef] [PubMed]
37. Angelucci, S.; Sacchetta, P.; Moio, P.; Melino, S.; Petruzzelli, R.; Gervasi, P.; Di Ilio, C. Purification and charac-terization of glutathione transferases from the sea bass (*Dicentrarchus labrax*) liver. *Arch. Biochem. Biophys.* **2000**, *373*, 435–441. [CrossRef]
38. Gallo, M.; Paludi, D.; Cicero, D.O.; Chiovitti, K.; Millo, E.; Salis, A.; Damonte, G.; Corsaro, A.; Thellung, S.; Schettini, G.; et al. Identification of a conserved N-capping box important for the structural autonomy of the prion alpha 3-helix: The disease associated D202N mutation destabilizes the helical conformation. *Int. J. Immunopathol Pharmacol.* **2005**, *18*, 95–112. [CrossRef]
39. Favaloro, B.; Tamburro, A.; Angelucci, S.; Luca, A.D.; Melino, S.; di Ilio, C.; Rotilio, D. Molecular cloning, expression and site-directed mutagenesis of glutathione S-transferase from *Ochrobactrum anthropi*. *Biochem. J.* **1998**, *335*, 573–579. [CrossRef] [PubMed]
40. Melino, S.; Nepravishta, R.; Bellomaria, A.; Di Marco, S.; Paci, M. Nucleic acid binding of the RTN1-C C-terminal region: Toward the functional role of a reticulon protein. *Biochemistry* **2009**, *48*, 242–253. [CrossRef]
41. Fazi, B.; Melino, S.; De Rubeis, S.; Bagni, C.; Paci, M.; Piacentini, M.; Di Sano, F. Acetylation of RTN-1C regulates the induction of ER stress by the inhibition of HDAC activity in neuroectodermal tumors. *Oncogene* **2009**, *28*, 3814–3824. [CrossRef]
42. Candi, E.; Agostini, M.; Melino, G.; Bernassola, F. How the TP53 family proteins TP63 and TP73 contribute to tumorigenesis: Regulators and effectors. *Hum. Mutat.* **2014**, *35*, 702–714. [CrossRef] [PubMed]
43. Tomasini, R.; Tsuchihara, K.; Tsuda, C.; Lau, S.K.; Wilhelm, M.; Rufini, A.; Tsao, M.S.; Iovanna, J.L.; Jurisicova, A.; Melino, G.; et al. TAp73 regulates the spindle assembly checkpoint by modulating BubR1 activity. *Proc. Natl. Acad. Sci. USA* **2009**, *106*, 797–802. [CrossRef]
44. Amelio, I.; Melino, G. The p53 family and the hypoxia-inducible factors (HIFs): Determinants of cancer progression. *Trends Biochem. Sci.* **2015**, *40*, 425–434. [CrossRef] [PubMed]
45. Candi, E.; Terrinoni, A.; Rufini, A.; Chikh, A.; Lena, A.M.; Suzuki, Y.; Sayan, B.S.; Knight, R.A.; Melino, G. p63 is upstream of IKK alpha in epidermal development. *J. Cell Sci.* **2006**, *119 Pt 22*, 4617–4622. [CrossRef]
46. Candi, E.; Cipollone, R.; Rivetti di Val Cervo, P.; Gonfloni, S.; Melino, G.; Knight, R. p63 in epithelial development. *Cell. Mol. Life Sci.* **2008**, *65*, 3126–3133. [CrossRef]
47. Bernassola, F.; Salomoni, P.; Oberst, A.; Di Como, C.J.; Pagano, M.; Melino, G.; Pandolfi, P.P. Ubiquitin-dependent degradation of p73 is inhibited by PML. *J. Exp. Med.* **2004**, *199*, 1545–1557. [CrossRef]
48. Scimeca, M.; Giocondo, R.; Montanaro, M.; Granaglia, A.; Bonfiglio, R.; Tancredi, V.; Mauriello, A.; Urbano, N.; Schillaci, O.; Bonanno, E. BMP-2 Variants in Breast Epithelial to Mesenchymal Transition and Microcalcifications Origin. *Cells* **2020**, *9*, 1381. [CrossRef]
49. Marchetti, P.; Antonov, A.; Anemona, L.; Vangapandou, C.; Montanaro, M.; Botticelli, A.; Mauriello, A.; Melino, G.; Catani, M.V. New immunological potential markers for triple negative breast cancer: IL18R1, CD53, TRIM, Jaw1, LTB, PTPRCAP. *Discov. Oncol.* **2021**, *12*, 6. [CrossRef]
50. Mancini, M.; Cappello, A.; Pecorari, R.; Lena, A.M.; Montanaro, M.; Fania, L.; Ricci, F.; Di Lella, G.; Piro, M.C.; Abeni, D.; et al. Involvement of transcribed lncRNA uc.291 and SWI/SNF complex in cutaneous squamous cell carcinoma. *Discov. Oncol.* **2021**, *12*, 14. [CrossRef] [PubMed]
51. Fraser, M.; Sabelnykova, V.Y.; Yamaguchi, T.N.; Heisler, L.E.; Livingstone, J.; Huang, V.; Shiah, Y.J.; Yousif, F.; Lin, X.; Masella, A.P.; et al. Genomic hallmarks of localized, non-indolent prostate cancer. *Nature* **2017**, *541*, 359–364. [CrossRef]
52. Armenia, J.; Wankowicz, S.A.M.; Liu, D.; Gao, J.; Kundra, R.; Reznik, E.; Chatila, W.K.; Chakravarty, D.; Han, G.C.; Coleman, I.; et al. The long tail of oncogenic drivers in prostate cancer. *Nat. Genet.* **2018**, *50*, 645–651. [CrossRef]

53. Zhou, K.; Arslanturk, S.; Craig, D.B.; Heath, E.; Draghici, S. Discovery of primary prostate cancer biomarkers using cross cancer learning. *Sci. Rep.* **2021**, *11*, 10433. [CrossRef] [PubMed]
54. REACCT Collaborative; Zaborowski, A.M.; Abdile, A.; Adamina, M.; Aigner, F.; d'Allens, L.; Allmer, C.; Álvarez, A.; Anula, R.; Andric, M.; et al. Characteristics of Early-Onset vs Late-Onset Colorectal Cancer: A Review. *JAMA Surg.* **2021**, *156*, 865–874, Erratum in *JAMA Surg.* **2021**, *156*, 894. [CrossRef]
55. cBioPortal Website. Available online: https://www.cbioportal.org/ (accessed on 27 January 2022).
56. Pierorazio, P.M.; Walsh, P.C.; Partin, A.W.; Epstein, J.I. Prognostic Gleason grade grouping: Data based on the modified Gleason scoring system. *BJU Int.* **2013**, *111*, 753–760. [CrossRef]
57. Gordetsky, J.; Epstein, J. Grading of prostatic adenocarcinoma: Current state and prognostic implications. *Diagn. Pathol.* **2016**, *11*, 25. [CrossRef] [PubMed]
58. Panatta, E.; Butera, A.; Celardo, I.; Leist, M.; Melino, G.; Amelio, I. p53 regulates expression of nuclear envelope components in cancer cells. *Biol. Direct* **2022**, *17*, 38. [CrossRef]
59. Wang, D.; Liufu, J.; Yang, Q.; Dai, S.; Wang, J.; Xie, B. Identification and validation of a novel signature as a diagnostic and prognostic biomarker in colorectal cancer. *Biol. Direct* **2022**, *17*, 29. [CrossRef] [PubMed]
60. Long, S.; Wang, Y.; Chen, Y.; Fang, T.; Yao, Y.; Fu, K. Pan-cancer analysis of cuproptosis regulation patterns and identification of mTOR-target responder in clear cell renal cell carcinoma. *Biol. Direct* **2022**, *17*, 28. [CrossRef] [PubMed]
61. Newell-Price, J.; Clark, A.J.; King, P. DNA methylation and silencing of gene expression. *Trends Endocrinol. Metab.* **2000**, *11*, 142–148. [CrossRef] [PubMed]
62. Shinawi, T.; Hill, V.K.; Krex, D.; Schackert, G.; Gentle, D.; Morris, M.R.; Wei, W.; Cruickshank, G.; Maher, E.R.; Latif, F. DNA methylation profiles of long- and short-term glioblastoma survivors. *Epigenetics* **2013**, *8*, 149–156. [CrossRef] [PubMed]
63. Men, C.; Chai, H.; Song, X.; Li, Y.; Du, H.; Ren, Q. Identification of DNA methylation associated gene signatures in endometrial cancer via integrated analysis of DNA methylation and gene expression systematically. *J. Gynecol. Oncol.* **2017**, *28*, e83. [CrossRef]
64. Irizarry, R.A.; Ladd-Acosta, C.; Wen, B.; Wu, Z.; Montano, C.; Onyango, P.; Cui, H.; Gabo, K.; Rongione, M.; Webster, M.; et al. The human colon cancer methylome shows similar hypo- and hypermethylation at conserved tissue-specific CpG island shores. *Nat. Genet.* **2009**, *41*, 178–186. [CrossRef] [PubMed]
65. Yang, C.F.; Hwu, W.L.; Yang, L.C.; Chung, W.H.; Chien, Y.H.; Hung, C.F.; Chen, H.C.; Tsai, P.J.; Fann, C.S.; Liao, F.; et al. A promoter sequence variant of ZNF750 is linked with familial psoriasis. *J. Investig. Dermatol.* **2008**, *128*, 1662–1668. [CrossRef] [PubMed]
66. Zhang, P.; He, Q.; Lei, Y.; Li, Y.; Wen, X.; Hong, M.; Zhang, J.; Ren, X.; Wang, Y.; Yang, X.; et al. Correction: m6A-mediated ZNF750 repression facilitates nasopharyngeal carcinoma progression. *Cell Death Dis.* **2022**, *13*, 83. [CrossRef]
67. Otsuka, R.; Akutsu, Y.; Sakata, H.; Hanari, N.; Murakami, K.; Kano, M.; Toyozumi, T.; Takahashi, M.; Matsumoto, Y.; Sekino, N.; et al. ZNF750 Expression Is a Potential Prognostic Biomarker in Esophageal Squamous Cell Carcinoma. *Oncology* **2018**, *94*, 142–148. [CrossRef] [PubMed]
68. Risbridger, G.P.; Davis, I.D.; Birrell, S.N.; Tilley, W.D. Breast and prostate cancer: More similar than different. *Nat. Rev. Cancer* **2010**, *10*, 205–212. [CrossRef]
69. Butera, A.; Roy, M.; Zampieri, C.; Mammarella, E.; Panatta, E.; Melino, G.; D'Alessandro, A.; Amelio, I. p53-driven lipidome influences non-cell-autonomous lysophospholipids in pancreatic cancer. *Biol. Direct* **2022**, *17*, 6. [CrossRef] [PubMed]
70. Sazonova, E.V.; Petrichuk, S.V.; Kopeina, G.S.; Zhivotovsky, B. A link between mitotic defects and mitotic catastrophe: Detection and cell fate. *Biol. Direct* **2021**, *16*, 25. [CrossRef]
71. Bonfiglio, R.; Nardozi, D.; Scimeca, M.; Cerroni, C.; Mauriello, A.; Bonanno, E. PD-L1 in immune-escape of breast and prostate cancers: From biology to therapy. *Future Oncol.* **2017**, *13*, 2129–2131. [CrossRef]
72. Salami, S.S.; Schmidt, F.; Laxman, B.; Regan, M.M.; Rickman, D.S.; Scherr, D.; Bueti, G.; Siddiqui, J.; Tomlins, S.A.; Wei, J.T.; et al. Combining urinary detection of TMPRSS2:ERG and PCA3 with serum PSA to predict diagnosis of prostate cancer. *Urol. Oncol.* **2013**, *31*, 566–571. [CrossRef]
73. Zappala, S.M.; Scardino, P.T.; Okrongly, D.; Linder, V.; Dong, Y. Clinical performance of the 4Kscore Test to predict high-grade prostate cancer at biopsy: A meta-analysis of us and European clinical validation study results. *Rev. Urol.* **2017**, *19*, 149–155. [CrossRef]
74. Erho, N.; Crisan, A.; Vergara, I.A.; Mitra, A.P.; Ghadessi, M.; Buerki, C.; Bergstralh, E.J.; Kollmeyer, T.; Fink, S.; Haddad, Z.; et al. Discovery and validation of a prostate cancer genomic classifier that predicts early metastasis following radical prostatectomy. *PLoS ONE* **2013**, *8*, e66855. [CrossRef]
75. Scimeca, M.; Bonfiglio, R.; Varone, F.; Ciuffa, S.; Mauriello, A.; Bonanno, E. Calcifications in prostate cancer: An active phenomenon mediated by epithelial cells with osteoblast-phenotype. *Microsc. Res. Tech.* **2018**, *81*, 745–748. [CrossRef]
76. Humphrey, P.A.; Moch, H.; Cubilla, A.L.; Ulbright, T.M.; Reuter, V.E. The 2016 WHO Classification of Tumours of the Urinary System and Male Genital Organs-Part B: Prostate and Bladder Tumours. *Eur. Urol.* **2016**, *70*, 106–119. [CrossRef]
77. Xie, M.; Gao, X.S.; Ma, M.W.; Gu, X.B.; Li, H.Z.; Lyu, F.; Bai, Y.; Chen, J.Y.; Ren, X.Y.; Liu, M.Z. Population-Based Comparison of Different Risk Stratification Systems Among Prostate Cancer Patients. *Front. Oncol.* **2021**, *11*, 646073. [CrossRef]
78. Liu, Y.; Chen, J.; Zhou, L.; Yin, C. LINC00885 promotes cervical cancer progression through sponging miR-3150b-3p and upregulating BAZ2A. *Biol. Direct* **2022**, *17*, 4. [CrossRef] [PubMed]

79. Qi, C.; Liu, J.; Guo, P.; Xu, Y.; Hu, J.; Han, X. LncRNA NORAD facilitates oral squamous cell carcinoma progression by sponging miR-577 to enhance TPM4. *Biol. Direct* **2022**, *17*, 1. [CrossRef] [PubMed]
80. Tang, Z.; Li, C.; Kang, B.; Gao, G.; Li, C.; Zhang, Z. GEPIA: A web server for cancer and normal gene expression profiling and interactive analyses. *Nucleic Acids Res.* **2017**, *45*, W98–W102. [CrossRef] [PubMed]
81. Cerami, E.; Gao, J.; Dogrusoz, U.; Gross, B.E.; Sumer, S.O.; Aksoy, B.A.; Jacobsen, A.; Byrne, C.J.; Heuer, M.L.; Larsson, E.; et al. The cBio cancer genomics portal: An open platform for exploring multidimensional cancer genomics data. *Cancer Discov.* **2012**, *2*, 401–404, Erratum in *Cancer Discov.* **2012**, *2*, 960. [CrossRef] [PubMed]
82. Gao, J.; Aksoy, B.A.; Dogrusoz, U.; Dresdner, G.; Gross, B.; Sumer, S.O.; Sun, Y.; Jacobsen, A.; Sinha, R.; Larsson, E.; et al. Integrative analysis of complex cancer genomics and clinical profiles using the cBioPortal. *Sci. Signal.* **2013**, *6*, pl1. [CrossRef] [PubMed]
83. Lánczky, A.; Győrffy, B. Web-Based Survival Analysis Tool Tailored for Medical Research (KMplot): Development and Implementation. *J. Med. Internet Res.* **2021**, *23*, e27633. [CrossRef] [PubMed]
84. Chandrashekar, D.S.; Bashel, B.; Balasubramanya, S.A.H.; Creighton, C.J.; Ponce-Rodriguez, I.; Chakravarthi, B.V.S.K.; Varambally, S. UALCAN: A Portal for Facilitating Tumor Subgroup Gene Expression and Survival Analyses. *Neoplasia* **2017**, *19*, 649–658. [CrossRef]
85. Chandrashekar, D.S.; Karthikeyan, S.K.; Korla, P.K.; Patel, H.; Shovon, A.R.; Athar, M.; Netto, G.J.; Qin, Z.S.; Kumar, S.; Manne, U.; et al. UALCAN: An update to the integrated cancer data analysis platform. *Neoplasia* **2022**, *25*, 18–27. [CrossRef] [PubMed]
86. Liu, C.; Kuang, J.; Wang, Y.; Duan, T.; Min, L.; Lu, C.; Zhang, T.; Chen, R.; Wu, Y.; Zhu, L. A functional reference map of the RNF8 interactome in cancer. *Biol. Direct* **2022**, *17*, 17. [CrossRef] [PubMed]
87. Sutter, M.; Kerfeld, C.A. BMC Caller: A webtool to identify and analyze bacterial microcompartment types in sequence data. *Biol. Direct* **2022**, *17*, 9. [CrossRef] [PubMed]